

OSCARKEMPFITE, $\text{Ag}_{10}\text{Pb}_4(\text{Sb}_{17}\text{Bi}_9)_{\Sigma 26}\text{S}_{48}$, A NEW Sb-Bi MEMBER OF THE LILLIANITE HOMOLOGOUS SERIES

Dan Topa^{1*}, Werner H. Paar², Emil Makovicky³, Chris J. Stanley⁴ and Andy C. Roberts⁵

¹Natural History Museum-Vienna, Burggring 7, A-1010 Vienna, Austria

²A-5020 Salzburg, Pezoltgasse 46, Austria

³Department of Geoscience and Resource Management, University of Copenhagen, Østervoldgade 10, DK-1350, Copenhagen K, Denmark,

⁴The Natural History Museum, Cromwell Road, London, SW7 5BD, England, UK

⁵Geological Survey of Canada, 601 Booth Street, Ottawa, Ontario K1A 0E8, Canada

*E-mail: dan.topa@sbg.ac.at

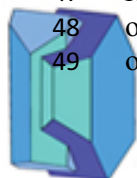
ABSTRACT

Oscarkempffite, ideally $\text{Ag}_{10}\text{Pb}_4(\text{Sb}_{17}\text{Bi}_9)_{\Sigma 26}\text{S}_{48}$, is a new mineral species found in old material (1929-30) from the Colorado vein, Animas mine, Chocaya Province, Department of Potosi, Bolivia. It is associated with aramayoite, stannite, miargyrite, pyrrargyrite, and freibergite. Oscarkempffite forms anhedral grains, and grain aggregates up to 10 mm across. The mineral is opaque, greyish black with a metallic luster; it is brittle without any discernible cleavage. In reflected light oscarkempffite is grayish white, pleochroism is distinct, white to dark grey. Internal reflections are absent. In crossed polars, anisotropism is distinct with rotation tints in shades of grey. The reflectance data (% air) are: 39.9, 42.6 at 470 nm, 38.6, 41.7 at 546 nm, 38.1, 41.2 at 589 nm and 37.3, 40.6 at 650 nm. Mohs hardness is 3-3½, microhardness VHN_{50} exhibits a range 189-208, with a mean value 200 kg mm^{-2} . The average results of four electron-microprobe analyses in a grain are: Cu 0.24(7), Ag 14.50(8), Pb 11.16(14), Sb 28.72(16), Bi 24.56(17), S 20.87(5), total 100.05(6) wt.%, corresponding to $\text{Cu}_{0.24}\text{Ag}_{9.92}\text{Pb}_{4.00}\text{Sb}_{17.36}\text{Bi}_{8.64}\text{S}_{47.84}$ (on the basis of $\text{Me} + \text{S} = 88 \text{ apfu}$). The simplified formula, $\text{Ag}_{10}\text{Pb}_4\text{Sb}_{17}\text{Bi}_9\text{S}_{48}$, is in accordance with the results of a crystal-structure determination. The density, 5.8 g/cm^3 , was calculated using the ideal formula. Oscarkempffite has an orthorhombic cell with $a = 13.199(2)$, $b = 19.332(3)$, $c = 8.249(1)$ Å, $V = 2116.3(5)$ Å³, space group $Pnca$, and $Z = 1$. The strongest eight lines in the (calculated) powder-diffraction pattern are [d in Å(I)(hkl)]: 3.66(35)(122), 3.37(70)(132), 3.34(100)(250), 2.982(55)(312), 2.881(86)(322), 2.733(29)(332), 2.073(27)(004) and 2.062(31)(182). Comparison with gustavite, andorite, and roshchinite confirms its independence as a mineral species.

Keywords: oscarkempffite, sulphosalt, new mineral, lillianite homologous series, Animas mine, Chocaya Province, Bolivia.

INTRODUCTION

The lillianite homologous series (Makovicky and Karup-Møller, 1977a, b) was defined for Pb-Bi-Ag sulfosalts although it was noticed already from the start that three antimony-based phases andorite, ramdohrite and fizelyite (Hellner, 1958) belonged to the same structural family. The andorite – ramdohrite branch of the lillianite series was subsequently studied in detail by Moëlo *et al.*, (1989). Phases belonging to the lillianite homologous series are composed of slabs of the slightly distorted PbS archetypal structure, cut and mirror-twinned on (113)_{PbS}. The octahedral coordinations present in the slabs are altered to bicapped prismatic coordinations on



50 the composition plane between adjacent slabs. Slab thickness can vary by increments of one or
51 more octahedra, measured diagonally across a slab. Number of octahedra along this diagonal
52 determines the order N of the homologue. Substitution [Ag + (Sb+Bi)]-for-2Pb is present in the
53 slabs but in most cases it does not involve the prismatic lead positions. For N = 4, relevant for
54 the present study, this substitution spans compositions from $Pb_3Bi_2S_6$ to $PbAg(Bi,Sb)_3S_6$,
55 expressed as the substitution percentage from 0 to 100%. The end-member composition
56 $Pb_3Sb_2S_6$ is unknown, both as a natural and a synthetic phase, and probably cannot exist as a
57 lillianite homologue. Cases of ‘oversubstitution’, in which also the prismatic position is
58 involved, are known, mostly for the antimony-based cases (Moëlo *et al.*, 1989). For N = 4, and a
59 Bi-based case, an orthorhombic *Bbmm* structure exists for substitutions of up to about 60%;
60 whereas a monoclinic *P2₁/c* superstructure is present for substitutions close to 100% (Makovicky
61 and Karup-Møller 1977b). The situation for the Sb-based phases is more complicated for the N =
62 4 line, with two highly substituted-to-oversubstituted phases (complicated 6-fold and 4-fold
63 superstructures of the basic lillianite scheme) and several moderately substituted cases present,
64 these often with other cations modifying the simple Pb-Ag-Sb scheme.

65 Studies of the *mixed antimony-bismuth members of the lillianite homologous series* were
66 first limited to a chemical characterization of them by means of electron microprobe analyses. It
67 was established (Mozgova *et al.*, 1987, Moëlo *et al.*, 1989) that extensive Bi-Sb substitution may
68 be present, straddling the 50:50 Sb:Bi divide, although typical gustavites and lillianites have low
69 contents of antimony (e.g., Makovicky and Topa, 2011, and the numerous references in Moëlo *et al.*,
70 1989). In a similar way, nearly all occurrences of andorite-ramdohrite homologues have only
71 low contents of bismuth (Moëlo *et al.*, 1989). Notable occurrences of mixed Sb-Bi phases are
72 Alyaskitovoye deposit (Yakutia, Russia) (Mozgova *et al.*, 1987), Flat Head (Montana, USA)
73 (Karup-Møller and Makovicky, unpublished), Julcani (Peru), El Mechero (Peru), Bazoges-en-
74 Paillers (Vendee, France) (all three by Moëlo *et al.*, 1987), and Kutná Hora (Central Bohemia,
75 Czech Republic) (Pažout *et al.*, 2001). Investigations of mixed phases were mostly hampered by
76 extreme variability of Sb:Bi ratios, often inside one aggregate or a needle-shaped grain, typical
77 for nearly all investigated occurrences. In spite of it, a successful crystal structure investigation
78 was performed by Pažout and Dušek (2009) on antimony-containing gustavite, $PbAgBi_2SbS_6$,
79 from the deposit of Kutná Hora, Czech Republic, with $a = 7.0455 \text{ \AA}$, $b = 19.5294 \text{ \AA}$, $c = 8.3412$
80 \AA , and $\beta 107.446^\circ$, space group *P2₁/c*. Another published structure of this category from Kutná
81 Hora is that of $Ag_{0.71}Pb_{1.52}Bi_{1.32}Sb_{1.45}S_6$, with $a = 4.254 \text{ \AA}$, $b = 13.309 \text{ \AA}$, $c = 19.625 \text{ \AA}$, space
82 group *Cmcm* (Pažout and Dušek, 2010). This orthorhombic phase has substitution percentage of
83 only 70.5%, according to the substitution scheme defined above (Makovicky and Karup-Møller,
84 1977a, b and Makovicky and Topa 2014).

85 The new investigation of the old material from the Colorada vein, Animas mine, Chocaya
86 Province, Department of Potosi, Bolivia (Ahlfeld and Reyes, 1938, Ahlfeld and Schneider-
87 Scherbina, 1964,) offered a chance to extend further the chemical range of investigated Sb-Bi
88 lillianite homologues with N = 4 and led to the definition of oscar Kempffite as a new species.

89 The mineral and its name have been approved by the CNMNC-IMA, under the number
90 IMA-2011-029 (Topa *et al.*, 2013). The name is in honor of Oscar Kempff Bacigalupo (1948-),
91 eminent Bolivian mineralogist and economic geologist, who discovered several large mineral
92 deposits in Bolivia (e.g., the deposit of Don Mario). The holotype specimen of oscar Kempffite is
93 deposited in the reference collection of the Naturhistorisches Museum Wien, Burgring 7, A-1010
94 Wien, Austria, with catalogue number N 9593. Cotype material is deposited in the reference
95 collection of the Natural History Museum, Cromwell Road, London SW7 5BD, United
96 Kingdom, with catalogue number BM 20, 3.

99 OCCURRENCE

100

101 Oscarkempffite has been determined in old samples which originate from the expeditions
102 of W. Vaux in 1929-30. The locality which is given on the labels associated with the two
103 specimens of this mineral, is Animas mine, Colorada vein. Chocaya is a typical deposit of the
104 Ag-Sn formation of Bolivia. Its geographical position is 66°33'W and 21°S. It is situated NW of
105 Atocha in the province of Sur Chicas, department of Potosi, Southern Bolivia, and thus very
106 close to the tectonic lineament which separates Paleozoic rocks of the Central Andes from the
107 high planes (= *altiplano*) of Bolivia. The vein-type Ag-Sn deposits occur NE of a volcanic stock
108 of dacitic rocks which has a diameter of 9 km and rises up against the Ordovician plane for more
109 than 900 meters. The volcanic rocks are strongly altered and propylitization, silicification and
110 pyritization are very common.

111 Colorada, which is the principal vein, follows a distinct fault zone for more than 1800 m
112 along strike. Other veins which parallel the Colorada structure are Arturo and Animas towards
113 W, and Burton and Judíos towards E. The Colorada vein has been exploited towards depth for
114 almost 750 m in the northern part and 600 m in the section of Animas in its southern part. In the
115 upper part of this vein cassiterite was associated with freibergite and members of the stannite-
116 k esterite family. Textures which clearly indicated open space filling have very distinct banding,
117 crustification and cockades.

118 At the Animas mine, some 70 m from the surface, an extremely rich ore shoot composed
119 of various minerals of silver was encountered during the exploitation of the mine. At a depth of
120 125 m, the ore shoot had a length of 30 m, a thickness of 2 m and the grade of silver was almost
121 3.5%. The principal silver mineral was freibergite. At the level -235 m the high-grade zone
122 contained the new mineral species aramayoite, Ag(Sb,Bi)₂, accompanied by stannite, miargyrite,
123 pyrargyrite, and freibergite. Aramayoite has been described in detail by Spencer and Mountain
124 (1926).

125 Oscarkempffite, the new sulfosalt species, is a typical associate of this assemblage
126 containing aramayoite. Though no details about the exact level are given on the labels associated
127 with the specimens, it can be assumed with certainty, that their origin is from the same level as
128 the discovery of aramayoite (-235 m level). The last and more important exploitation at the
129 Animas mine stopped in 1961, when significant amounts of Pb, Ag, Sn and Zn were mined.
130 However, small-scale mining by local mining communities (“cooperativas”) at the deeper levels
131 of the Animas mine was still going on at the time of the last visit of one of the authors (WHP,
132 2004) and probably continues to the present day.

133

134 MINERAL ASSOCIATION

135

136 Oscarkempffite forms anhedral grains attaining a size of up to several mm and grain
137 aggregates ranging up to 10 mm across. A BSE photograph (Fig. 1a) of such an aggregate shows
138 differences in the contents of cations with high Z values as smooth zoning with a higher average
139 Z in the centre. The same aggregate in reflected light (Fig. 1b) displays an irregular mosaic
140 character and pronounced anisotropy. Surrounding association is not visible because of high
141 contrast. Figure 1c shows a large field of Ag-bearing tetrahedrite with another, silver richer
142 (lighter on the BSE image) generation deposited in a void and irregular grains of oscarkempffite
143 that penetrate into tetrahedrite on the boundary and enclose a small aramayoite grain. The
144 complex round sulphide aggregate in Figure 1d is interpreted as a replacement of an old
145 unknown precursor mineral (aggregate) of approximately round shape by oscarkempffite (a
146 ‘wreath’ of light grains and a grain in the centre) cemented by a large grain of bismuth-rich
147 aramayoite (lighter grey) and another of less bismuthian aramayoite variety (slightly darker grey,
148 lower left-hand parts). Small crystals of quartz and a grain of tetrahedrite with a ‘cap’ of Ag-
149 enriched tetrahedrite variety (dark grey on the BSE image) are enclosed. Close to the lower
150 corners of the figure, dark semi-decomposed grains of stannite are present. Oscarkempffite
151 overgrew/replaced the original aggregate from the outside and later also the remaining old grain.

152 Much of oscarkeppffite was subsequently replaced by aramayoite. Stannite apparently predates
153 aramayoite, as seen in the lower right-hand corner.

154

155 PHYSICAL PROPERTIES

156

157 The colour of the mineral is greyish black, streak dark grey; it is opaque with metallic
158 luster, non-fluorescent. H(Mohs) is 3-3½, microhardness VHN₅₀ is ranging between 189 and 208,
159 with a mean value 200 kg mm⁻². The mineral is brittle with irregular fracture; no cleavage or
160 parting are observed. Density could not be measured because of paucity of available material.
161 Calculated density is 5.8 g cm⁻³ using the empirical formula. No crystal forms and twinning of
162 the anhedral grains and aggregates were observed. The *a:b:c* ratio calculated from the unit-cell
163 parameters (see below) is 0.683:1:0.429.

164

165 OPTICAL PROPERTIES

166

167 In reflected light (plane polars) the colour of oscarkeppffite is grayish white.
168 Pleochroism is distinct, white to dark grey; bireflectance is weak to distinct (in oil); no internal
169 reflections were detected. With crossed polars, anisotropism is distinct with rotation tints in
170 shades of grey. Reflectance values in air and oil, (The Natural History Museum, London, UK,
171 WTiC standard, refractive index of oil: 1.515 at 23°C) are given in Table 1. A slight, fairly even
172 decrease of reflectance with increasing wavelength is observed.

173

174 CHEMICAL DATA

175

176 Chemical analyses of oscarkeppffite (Table 2) were carried out using an electron
177 microprobe JEOL JXA-8600, installed at University of Salzburg, Austria, (WDS mode, 25 kV,
178 20 nA, 5 µm beam diameter, ZAF correction procedure). Other elements (Hg, Tl and As) were
179 sought but not detected. The standards and wavelengths used are chalcopyrite (nat.) CuKα,
180 FeKα, shalerite (nat.) ZnKα, metal (syn.) AgLα, galena (nat.) PbLα, stibnite (nat.) SbLα and
181 bismuthinite (syn.) BiLα and SKα. Data for oscarkeppffite and associated minerals are
182 presented in Table 2.

183 The empirical formula of oscarkeppffite varies between (Ag,Cu)_{9.88}Pb_{4.40}Sb_{18.0}Bi_{7.44}S_{48.32}
184 and (Ag,Cu)_{10.24}Pb_{3.68}Sb_{16.40}Bi_{9.44}S_{48.32}. It is very close to the simplified formula
185 Ag₁₀Pb₄(Sb₁₇Bi₉)₂₆S₄₈. The crystal structure defines oscarkeppffite as a lillianite homologue
186 with the order N = 4. The cation ratios resulting from the chemical analysis confirm this
187 assignment, yielding N = 4.07 – 4.09. With respect to the measure of [Ag + (Bi,Sb)] ↔ 2Pb
188 substitution, typical for the lillianite-gustavite and fizelyite-andorite substitution lines (both N =
189 4), oscarkeppffite is heavily over-substituted, with a substitution percentage of 120 - 124%.

190 Chemical analyses (Table 2) of aggregates shown in Figure 1d represent three groups of
191 oscarkeppffite chemistries and two types of tetrahedrite illustrated, among which the one richest
192 in Ag represents the minor later phase (Fig. 1c). Among the three analyses of aramayoite, nos. 3
193 and 4 represent the aggregate in Figure 1d, no. 5 another aggregate. In conclusion, they show a
194 substantial variability of the Sb/Bi ratio.

195

196 CRYSTALLOGRAPHY

197 A diffractometer with an area detector system was used to perform the single-crystal study
198 (University of Salzburg, Austria). Cell parameters refined from single-crystal data are as follows:
199 orthorhombic system, space group *Pnca*, *a* = 13.199(2) Å, *b* = 19.332(3) Å, *c* = 8.294(1) Å, cell
200 volume *V* = 2116.3(5) Å³, and *Z* = 1 for the above formula unit.

201 Powder X-ray data were collected using a 114.6 mm diameter Debye-Scherrer camera
202 (Cu radiation, Ni filter, $CuK\alpha = 1.54178 \text{ \AA}$). Data are presented in Table 3. The calculated
203 powder data from results of the single-crystal study are shown in Table 4. Cell parameters
204 refined from the powder data are as follows: $a = 13.240(5) \text{ \AA}$, $b = 19.339(7) \text{ \AA}$, $c = 8.320(4) \text{ \AA}$,
205 and $V = 2130(2) \text{ \AA}^3$, in fair agreement with the single-crystal data.
206

207 CRYSTAL STRUCTURE

208 A fragment with irregular shape and 0.15 x 0.05 x 0.05 mm in size was mounted and
209 analyzed on a Bruker AXS three-circle diffractometer equipped with a CCD area detector.
210 The structure of oscarkempffite contains five distinct coordination polyhedra of cations and
211 seven of anions. It contains a mixed (Pb,Bi) site with a trigonal prismatic coordination, a silver
212 site with a distorted tetrahedral coordination in an octahedral arrangement of ligands, which
213 alternates along the 8 \AA direction with a mixed ($Sb_{0.88}Bi_{0.12}$) site called Sb1, and a string of
214 alternating Sb2 and a mixed ($Sb_{0.59}Bi_{0.41}$) sites, the latter called Sb3, in the central parts of PbS-
215 like slabs. When proceeding along [100], the arrangement of consecutive atomic planes differs
216 from that in the monoclinic gustavite structure, resulting in orthorhombic symmetry and in –Sb-
217 Sb-Ag-Ag-Sb-Sb- zig-zag [010] chains of coordination octahedra instead of the Ag-Bi-Ag-Bi-
218 chains present in gustavite. The crystal structure is shown in Figure 2.

219 Details of the crystal structure and the interesting geometric relationships between the
220 structures of orthorhombic oscarkempffite and monoclinic gustavite $PbAgBi_3S_6$ are treated in a
221 parallel paper (Topa and Makovicky, submitted).
222

223 RELATION TO OTHER SPECIES

224

225 Oscarkempffite is essentially a pure Ag-(Sb, Bi)-Pb sulfosalt with only trace amounts of
226 copper and without As. It is a lillianite homologue $N = 4$ as confirmed by the N value calculated
227 from the chemical analysis. With respect to the measure of $(Ag + Bi) \leftrightarrow 2Pb$ substitution, typical
228 of the lillianite-gustavite and fizelyite-andorite substitution lines, oscarkempffite is heavily
229 oversubstituted, with a substitution percentage of 124%, far beyond the 100% value of gustavite,
230 $PbAgBi_3S_6$ (Makovicky and Karup-Møller, 1977a,b) and the ~100% value of senandorite
231 (andorite VI; Sawada *et al.*, 1987). In this, it resembles the partly heterogeneous ‘bismuthian
232 andorites’ from Julcani, Peru, analysed by Mořlo *et al.*, (1989) without crystallographic studies.
233 They are distinguished by higher contents of copper, constant presence of arsenic (mostly
234 between 1.2 and 2.5 wt. %), substitution percentages between ~101 and 119% and very variable
235 Sb:Bi ratios (Mořlo *et al.*, 1989).

236 The orthorhombic Sb-Bi member of the lillianite homologous series from Kutná Hora
237 (Czech Republic), investigated by Pařout and Duřek (2010) has the composition
238 $Ag_{0.71}Pb_{1.52}Bi_{1.32}Sb_{1.45}S_6$. It has substitution percentage of only 70.5% and its lattice, with $a =$
239 4.254 \AA , $b = 13.309 \text{ \AA}$, $c = 19.625 \text{ \AA}$, space group *Cmcm*, corresponds to a classical unit cell of
240 lillianite. Oscarkempffite also resembles roshchinite (Spiridonov *et al.*, 1990) from Kvarcituve
241 Gorki deposit, Kazakhstan, for which published data indicate a substitution value of 120%. In
242 roshchinite, however, Bi is absent, As is present in 3.5 wt. %, and the crystal structure has not
243 been worked out beyond the subcell of andorite type (Petrova *et al.*, 1986). Comparative data for
244 oscarkempffite and related minerals are given in Table 5.
245

246

247 ACKNOWLEDGEMENTS

248 We appreciate very much the information about the geology at Chocaya communicated
249 by Dr. Sohrab Tawackoli, La Paz. The two specimens containing the new species were provided
250 by Dr. Rob Lavinsky (Arkenstone). They were originally part of the famous Philadelphia
251 collection which contained a lot of historically important materials. The paper was handled
252 by.....and the comments of Dr. Nigel Cook and an anonymous referee helped to improve the
253 paper.
254

255

256 REFERENCES

257

258 Ahlfeld, F. and Reyes, J.M. (1938) Mineralogie von Bolivien. Berlin, Verlag: Gebrüder
259 Borntraeger, 90p.

260

261 Ahlfeld, F. and Schneider-Scherbina, A. (1964) Los yacimientos minerales y de hidrocarburos de
262 Bolivia. *Boletín de Departamento Nacional de Geología del Ministerio de Minas y Petroléo*, **5**,
263 (*Especial*), La Paz, 388 p.

264

265 Hellner, E. (1958) A structural scheme for sulfide minerals. *J.Geol.* **66**, 503-525.

266

267 Kraus, W. and Nolze, G. (1999) *PowderCell 2.3*. Federal Institute for Materials Research
268 and Testing, Berlin, Germany.

269

270 Makovicky, E. and Karup-Møller, S. (1977a) Chemistry and crystallography of the lillianite
271 homologous series. Part 1. General properties and definitions. *Neues Jahrbuch für Mineralogie*,
272 *Abhandlugen*, **130**, 264-287.

273

274 Makovicky, E. and Karup-Møller, S. (1977b) Chemistry and crystallography of the lillianite
275 homologous series. Part 2. Definition of new minerals: eskimoite, vikingite, ourayite and
276 treasurite. Redefinition of schirmerite and new data on the lillianite-gustavite solid-solution
277 series. *Neues Jahrbuch für Mineralogie, Abhandlugen*, **131**, 56-82.

278

279 Makovicky, E. and Topa D. (2011) The crystal structure of gustavite, $\text{PbAgBi}_3\text{S}_6$. Analysis
280 of twinning and polytypism using the OD approach. *European Journal of Mineralogy*
281 **23**, 537-550.

282

283 Makovicky, E. and Topa D. (2014) Lillianites and andorites: new life for the oldest homologous
284 series of sulphosalts. *Mineralogical Magazine*, **78**, 387-414.

285

286 Moëlo, Y., Makovicky, E. and Karup-Møller, S. (1989) Sulfures complexes plombo
287 argentifères : minéralogie et cristalochimie de la série andorite-fizélyite,
288 $(\text{Pb,Mn,Fe,Cd,Sn})_{3-2x}(\text{Ag,Cu})_x(\text{Sb,Bi,As})_{2+x}(\text{S,Se})_6$. *Documents du BRGM*, **167**, 1-107.

289

290 Pažout, R. and Dušek, M. (2009) Natural monoclinic $\text{AgPb}(\text{Bi}_2\text{Sb})_3\text{S}_6$, an Sb-rich gustavite.
291 *Acta Crystallographica*, **C65**(11), 177-180.

292

293 Pažout, R. and Dušek, M. (2010) Crystal structure of natural orthorhombic
294 $\text{Ag}_{0.71}\text{Pb}_{1.52}\text{Bi}_{1.32}\text{Sb}_{1.45}\text{S}_6$, a lillianite homologue with $N = 4$; comparison with gustavite.
295 *European Journal of Mineralogy* **22**, 741-750.

296

297 Petrova, I.V., Pobedimskaya, E.A. and Spiridonov, E.M. (1986) Crystal structure of roshchinite.
Materialy X. Vsesoyuz. Sov. po Rentgenografii Mineral'nogo Syrya, Tbilisi, 99-100 (in Russian).

298

299 Sawada, H., Kawada, I., Hellner, E. and Tokonami, M. (1987) The crystal structure of
300 senandorite (andorite VI): $PbAgSb_3S_6$. *Zeitschrift für Kristallographie* **180**, 141-150.

301

302 Spencer, L.J. and Mountain, E.D. (1926) Aramayoite, a new mineral from Bolivia.
303 *Mineralogical Magazine*, **21**, 156-162.

304

305 Spiridonov, E.M., Petrova, I.V., Dashevskaya, D.M., Balashov, E.P. and Klimova, L.M.
306 (1990) Roshchinite, $Pb_{10}Ag_{19}Sb_{51}S_{96}$ – a new mineral. *Doklady Akademii Nauk SSSR*,
307 **312**, 197-200.

308

309 Topa, D., Makovicky, E., Paar, W.H., Stanley, C.J. and Roberts, A.C. (2011) Oscarkempffite,
310 IMA 2011-029. CNMNC Newsletter No. 10, October 2011, page 2607; *Mineralogical*
311 *Magazine*, **75**, 2601-2613.

312

313

314

315

316

317

FIGURE CAPTIONS

318

Fig. 1. (a) A BSE photograph of an aggregate of oscarkempffite shows differences in the
319 contents of cations with high Z values as smooth zoning with a higher average Z in the centre.

320

(b) The same aggregate in reflected light displays an irregular mosaic character and pronounced
321 anisotropy. Associated with pyrite. (c) A large field of Ag-bearing tetrahedrite with another, still
322 silver richer (lighter) generation deposited in a void. Irregular grains of oscarkempffite penetrate
323 into tetrahedrite on the boundary and enclose a small aramayoite grain. (d) A complex round
324 sulfide aggregate interpreted as a replacement of an old unknown mineral aggregate.

325

Oscarkempffite (a 'wreath' of light grains and a grain in the centre) is corroded and cemented by
326 a later, large grain of Bi-rich aramayoite (lighter grey) and another grain of Bi-poorer aramayoite
327 (slightly darker grey, left-hand parts). Small crystals of quartz and a grain of tetrahedrite with a
328 'cap' of Ag-enriched tetrahedrite (dark grey) are enclosed. At lower corners of the figure, dark
329 semi-decomposed grains of stannite are present. Interpretation in the text.

330

331

Fig. 2. Cation and anion sites in the crystal structure of oscarkempffite. Unit cell is projected on
332 (001). In the order of decreasing size spheres indicate: S, (Pb,Bi) (grey), (Sb,Bi) (white) and Ag
333 (black). The $(311)_{PbS}$ slabs of PbS-like arrangement are perpendicular to [010]; they are
334 separated by (010) planes occupied by trigonal coordination prisms of (Pb,Bi).

335

Table 1. Reflectance values in air and oil (WTiC standard, refractive index of oil: 1.515 at 23°C) for oscar Kempffite.

λ (nm)	air		oil		λ (nm)	air		oil	
	R_{min}	R_{max}	R_{min}	R_{max}		R_{min}	R_{max}	R_{min}	R_{max}
400	41.6	44.4	26.0	41.6	560	38.4	41.5	22.4	38.4
420	40.8	43.6	25.4	40.8	580	38.1	41.3	22.2	38.1
440	40.5	43.2	24.7	40.5	589	38.1	41.2	22.1	38.1
460	40.1	42.7	24.3	40.1	600	38.0	41.1	22.0	38.0
470	39.9	42.6	24.1	39.9	620	37.7	40.8	21.7	37.7
480	39.7	42.5	23.8	39.7	640	37.4	40.7	21.7	37.4
500	39.4	42.2	23.5	39.4	650	37.3	40.6	21.4	37.3
520	39.0	42.0	23.1	39.0	660	37.1	40.4	21.3	37.1
540	38.7	41.7	22.7	38.7	680	36.9	40.2	21.1	36.9
546	38.6	41.7	22.6	38.6	700	36.8	39.9	21.1	36.8

Table 2. Analytical results for oscarkempffite and associated minerals.

Nr.	Mineral	NA	Cu	Ag	Fe	Zn	Pb	Sb	Bi	S	total
1	tetrahedrite	16	23.99(30)	19.97(20)	5.64(12))	0.87(13))	-	26.39(39)	-	23.00(14)	99.86(30)
2	tetrahedrite	3	17.38(24)	28.63(01)	4.98(31)	1.34(19)	-	25.55(06)	-	22.18(12)	100.06(04)
3	aramayoite	3	-	34.26(23)	-	-	-	27.70(33)	17.50(44)	20.06(09)	99.52(21)
4	aramayoite	3	-	35.26(28)	-	-	-	30.55(19)	13.48(25)	20.53(03)	99.82(11)
5	aramayoite	3	-	36.34(12)	-	-	-	36.83(68)	5.45(56)	21.05(07)	99.67(11)
6	oscarkempffite	5	0.35(07)	13.98(19)	-	-	12.56(77)	30.13(49)	21.41(20)	21.33(12)	99.76(13)
7	oscarkempffite	4	0.24(03)	14.50(08)	-	-	11.16(14)	28.72(16)	24.56(17)	20.87(05)	100.05(06)
8	oscarkempffite	4	0.29(04)	14.48(08)	-	-	10.03(36)	27.12(40)	26.73(37)	21.04(15)	99.96(32)

The data are expressed in wt.%. NA = Number of analyses. Formulae are calculated on the basis of $\Sigma(Me+S) = 29$ *a.p.f.u.* for tetrahedrite, 24 *a.p.f.u.* for aramayoite, and 88 *a.p.f.u.* for oscarkempffite, respectively. N_{chemical} and Ag_{subst} are calculated as described in Makovicky and Topa (2014).

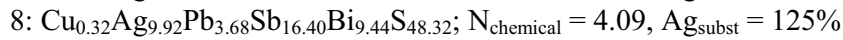
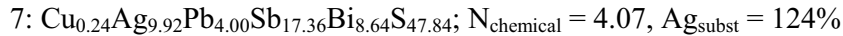
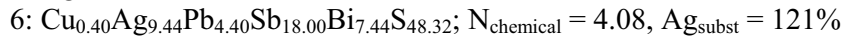
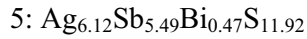
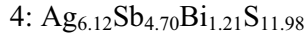
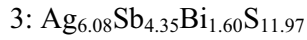
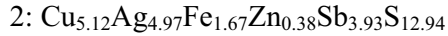
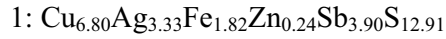


Table 3. X-ray powder diffraction data for oscar Kempffite.

$I_{rel.}$	$d_{meas}/\text{\AA}$	$d_{calc}/\text{\AA}$	h	k	l
5	6.292	6.263	2	1	0
5	5.463	5.463	2	2	0
20*	3.904	3.904	2	4	0
30*	3.663	3.672	1	2	2
		3.380	1	3	2
100b	3.354	3.340	2	5	0
20*	3.264	3.263	4	1	0
5	3.053	3.068	1	4	2
40*	2.988	2.991	3	1	2
80*	2.889	2.889	3	2	2
30*	2.741	2.740	3	3	2
10*	2.551	2.550	2	7	0
5*	2.417	2.417	0	8	0
40*	2.263	2.267	1	7	2
20*	2.112	2.111	5	3	2
		2.073	0	0	4
60	2.066	2.062	1	8	2
30*	2.027	2.028	5	4	2
30*	2.008	2.008	6	4	0
		1.933	0	10	0
30	1.931	1.930	5	5	2
20*	1.890	1.889	3	8	2
10*	1.834	1.836	5	6	2
5*	1.803	1.802	4	9	0
50*b	1.766	1.766	2	5	4
10*	1.722	1.722	7	0	2

*Lines used for unit cell refinement. Indexed on a 13.240(5), b 19.339(7), c 8.320(4) Å; refined on 17 reflections, between 3.904 and 1.772 Å, for which unambiguous indexing was possible, based on the calculated powder pattern derived from the successful determination of the crystal structure; intensities were estimated visually; b = broad line; the pattern was not corrected for shrinkage and no internal standard was used.

Table 4. Calculated X-ray powder diffraction data for oscar Kempffite.*

<i>I</i> _{rel.}	<i>d</i> _{calc} /Å	<i>h</i>	<i>k</i>	<i>l</i>	<i>I</i> _{rel.}	<i>d</i> _{calc} /Å	<i>h</i>	<i>k</i>	<i>l</i>
8	6.25	2	1	0	31	2.062	1	8	2
10	5.45	2	2	0	29	2.023	5	4	2
20	3.90	2	4	0	16	2.002	6	4	0
35	3.66	1	2	2	9	1.9332	0	10	0
70	3.37	1	3	2	9	1.9297	5	5	2
100	3.34	2	5	0	14	1.8863	3	8	2
15	3.30	4	0	0	8	1.8319	5	6	2
22	3.25	4	1	0	5	1.8002	4	9	0
6	3.22	0	6	0	24	1.7610	2	5	4
55	2.982	3	1	2	5	1.7556	4	0	4
25	2.895	2	6	0	5	1.7500	3	9	2
86	2.881	3	2	2	5	1.7484	4	1	4
29	2.733	3	3	2	6	1.7165	7	0	2
5	2.548	2	7	0	6	1.6858	2	6	4
21	2.265	1	7	2	6	1.6680	4	10	0
13	2.105	5	3	2	6	1.6264	8	2	0
5	2.082	6	3	0	7	1.4403	6	4	4
27	2.073	0	0	4	5	1.4140	0	10	4

*The theoretical pattern was calculated with PowderCell 2.3 software (Kraus and Nolze, 1999) in Debye-Scherrer configuration employing CuK α radiation ($\lambda = 1.540598$ Å), a fixed slit, and no anomalous dispersion. Cell parameters, space group, atom positions, site-occupancy factors and isotropic displacement factors from the crystal-structure determination were used.

Table 5. Comparative data for oscar Kempffite and related minerals.

Mineral	oscar Kempffite	gustavite ¹	andorite VI ²	roshchinite ³
Formula	Ag ₁₀ Pb ₄ Sb ₁₇ Bi ₉ S ₄₈	Ag ₄ Pb ₄ Bi ₉ Sb ₃ S ₂₄	Ag ₆ Pb ₆ Sb ₁₈ S ₃₆	Ag _{9.5} Pb ₅ Sb _{25.5} S ₄₈
Substitution (%)	124	100	100	120
Crystal system	orthorhombic	monoclinic	orthorhombic	orthorhombic
Space group	<i>Pnca</i>	<i>P2₁/c</i>	<i>Pn2₁a</i>	<i>Pmna</i>
Cell parameters (Å)				
<i>a</i>	13.199	7.046	13.005	12.946
<i>b</i>	19.332	19.529	19.155	19.048
<i>c</i>	8.294	8.342	25.622	16.932
α, β, γ (°)	90, 90, 90	90, 107.45, 90	90, 90, 90	90, 90, 90
<i>Z</i>	1	1	1	2
<i>R_I</i> factor (%)	3.7	5.88	4.89	-
Ref ⁴ .	1	2	3	4,5

¹Also gustavite with less Sb substitution, Ag₄Pb₄Bi_{11.2}Sb_{0.8}S₂₄, with *a* = 7.056, *b* = 9.691, *c* = 8.222 Å, β = 106.9°, space group *P2₁/c*, *R_I* = 2.76%, by Makovicky and Topa (2011). ²Or senandorite. ³Tentative crystal structure refinement of Petrova *et al.* (1986). ⁴[1]: this study; [2]: Pažout & Dušek (2010); [3]: Sawada *et al.* (1987); [4]: Spiridonov *et al.* (1990); [5]: Petrova *et al.* (1986).

